TISSUE ENGINEERING. PART A
Mary Ann Liebert, Inc. publishers
Journals Search Alerts

Tissue Eng Part A. 2012 Feb; 18(3-4): 423–431. PMCID: PMC3267967
Published online 2011 Oct 25. doi: 10.1089/ten.tea.2010.0677 PMID: 21919799

Measurements of the Effects of Decellularization on Viscoelastic Properties of Tissues in Ovine, Baboon, and Human Heart Valves

Tong Jiao, Ph.D.,[1] Rodney J. Clifton, Ph.D.,[1] Gabriel L. Converse, Ph.D.,[2] and Richard A. Hopkins, M.D.[2]

[1]School of Engineering, Brown University, Providence, Rhode Island.
[2]Cardiovascular Research Institute, Children's Mercy Hospital, Kansas City, Missouri.
Corresponding author.
Address correspondence to: *Tong Jiao, Ph.D., School of Engineering, Brown University, Box. D, Engineering, 182 Hope St., Providence, RI 02912. E-mail:*tong_jiao@brown.edu

Received 2010 Nov 22; Accepted 2011 Sep 15.

Abstract

In the development of tissue-engineered heart valves based on allograft decellularized extracellular matrix scaffolds, the material properties of the implant should be ideally comparable to the native semilunar valves. This investigation of the viscoelastic properties of the three functional aortic/pulmonary valve tissues (leaflets, sinus wall, and great vessel wall) was undertaken to establish normative values for fresh samples of human valves and to compare these properties after various steps in creating scaffolds for subsequent bioreactor-based seeding protocols. Torsional wave methods were used to measure the viscoelastic properties. Since preclinical surgical implant validation studies require relevant animal models, the tests reported here also include results for three pairs of both ovine and baboon aortic and pulmonary valves. For human aortic valves, four cryopreserved valves were compared with four decellularized scaffolds. Because of organ and heart valve transplant scarcity for pulmonary valves, only three cryopreserved and two decellularized pulmonary valves were tested. Leaflets are relatively soft. Loss angles are similar for all tissue samples. Regardless of species, the decellularization process used in this study has little effect on viscoelastic properties.

Introduction

MOST EXISTING REPORTS on the mechanical response of cardiovascular materials are focused on their response under tension and flexure.[1–15] Among them, only a few investigations report the time-dependent or viscoelastic mechanical properties of heart valves tissues.[5,6,12,15] There are even fewer reports on the viscoelastic shear properties of heart valve tissues. Especially for leaflets, because of their multilayer structure, understanding their viscoelastic shear properties is very important. Efforts to tissue-engineer heart valve tissues have led to investigations of the biomechanical properties of decellularized heart valve tissues. However, there are no systematic measurements of the viscoelastic properties of heart valve tissues and the comparison of their shear properties before and after decellularization.

To obtain the viscoelastic shear properties of heart valve tissues, both before and after decellularization, we have used the recently developed torsional wave facility at Brown University to measure the viscoelastic properties of native and acellular, aortic and pulmonary valves of sheep, baboons, and humans. By employing high frequencies, the highly frequency-dependent characteristics that "tune" the cardiovascular system in the range of expected heart rates (e.g., 1–3 Hz) can be avoided, thereby simplifying tissue comparisons.[16–18]

To determine whether any animal model might be relevant to human models for preclinical research, this study includes tests of the viscoelastic properties of aortic/pulmonary valve tissues from ovine and baboon.

The objectives are (1) to obtain measurements of the viscoelastic properties of species-specific native tissues, (2) to investigate whether decellularization causes degradation of the material properties that might preclude this approach for creating scaffolds for tissue-engineered valves, and (3) to compare human valves to valves from a subhuman primate and a food stock ungulate.

Materials and Methods

Experimental design and sample preparation

To establish normative values of the viscoelastic properties of all components of the semilunar heart valves, and to evaluate the consequences of the process of decellularization, measurement is made before and after decellularizing allograft semilunar heart valves to create extracellular matrix (ECM) scaffolds. Table 1 summarizes the experiments that have been done. The initial tests reported here include results for three pairs of aortic and pulmonary valves for both ovine and baboon and four cryopreserved and three decellularized aortic valves for human. As the human pulmonary valves are hard to acquire because of their clinical need, only four cryopreserved and two decellularized human valves were tested. Including the results for another one or two decellularized pulmonary valves from humans would strengthen the conclusions. However, from the statistical analysis, it was found that—provided the power is 80% with the given number of samples—the difference between the real values and the measured mean values of the viscoelastic properties of tissues from the decellularized human pulmonary valve is much smaller than one standard deviation.

Table 1.

Summary of the Number of Valves Investigated

	Fresh/cryopreserved		*Decellularized*	
	AV	***PV***	***AV***	***PV***
Ovine	3	3	3	3
Baboon	3	3	3	3
Human	4	4	3	2

Only human samples were cryopreserved.

AV, aortic valve; PV, pulmonary valve.

It is well known that vascular structures, including valves, typically lose compliance with age because of adaptive remodeling in response to increased stresses such as hypertension or pathological processes such as degenerative valve disease. Because this pilot study is focused on the general viscoelastic properties of tissues from aortic and pulmonary valves, comparison between age and gender of the samples are not main factors investigated in this report. Therefore, the cryopreserved human samples are selected from adults of either gender and are limited by availability of these gifted tissues to valves not useable clinically because of minor imperfections or inability to clear strict donor criteria. Table 2 gives the age and gender for the human samples.

Table 2.

Age and Gender of the Human Samples

Sample No.	*Type*	*Donor ID*	*Age (years)*	*Gender*
1	AV	05-4825	20	F
2	AV	04-2155	30	M
3	AV	02-4709	—	—
4	AV	02-3485	37	F
5[a]	AV	CSKC-09-06	48	F
7[a]	AV	CSKC-10-36	52	M
8[a]	AV	CSKC-09-157	48	F
9	PV	07-0442	20	M
10	PV	06-4709	23	M
11	PV	07-5184	25	F
12	PV	07-5378	41	F
13[a]	PV	09-3225	39	M
14[a]	PV	08-2606	46	M

[a]Decellularized sample.

Fresh hearts from sheep and baboons were cleanly harvested and sent in antibiotic saline on ice to our laboratory (24 h). The valves were then dissected in a manner similar to homograft valve recovery. Valves were kept in lactated ringer's solution, with antibiotics, at 4°C for up to 72 h before testing. Human samples were provided by LifeNet Health (LNH). They were cryopreserved in a freezing chamber at the controlled cooling rate of −1°C per minute, utilizing a programmable controller to a specific endpoint (−40°C or cooler). The allograft was then transferred to permanent storage in vapor-phase liquid nitrogen.[18] The cryopreserved human samples were shipped to our lab from LNH in a cryoshipper, which can keep the sample frozen in the vapor of liquid nitrogen for 3 or 4 days. To remove the dimethylsulfoxide from the cryopreserved sample without damaging the tissues, the clinically validated thawing process was used.[17]

Intact valves were decellularized using methods previously described.[19] Briefly, valves were treated with two cycles of reciprocating hypo/hyper osmolality to fracture cell membranes and then extracted with a nonionic detergent (Triton X-100, 0.05%, v/v; Sigma-Aldrich), followed by treatment with recombinant endonuclease (Benzonase; EMD Chemicals). Valves were further subjected to separate treatments in an anionic detergent (*N*-lauroylsarcosine, 1.0%, v/v; Sigma-Aldrich) and ethanol (40%, v/v; Sigma-Aldrich). Extraction of organic solvents was then performed using ion exchange resins (Amberlite XAD 16, Dowex Monosphere 550A Biobeads, IWT-TMD-8; Sigma-Aldrich).

Aortic valves and pulmonary valves are morphologically similar. They both function by the opening and closing of three nonmuscular flaps (cusps), called leaflets. Each leaflet responds to the deformation of a thinned region of the vessel wall, called the sinus. The vessel wall above the sinus is called the great vessel wall. For each aortic/pulmonary valve, cylindrical samples were obtained by dermal punch from each of three leaflets, three sinuses, and three positions on the great vessel wall. For each leaflet/sinus/great vessel wall, three samples are cored out (for some valves, the leaflets and sinuses are too small to obtain three samples, so two samples are cored). Figure 1 shows the cryopreserved human aortic/pulmonary valve and the positions where the cylindrical specimens were sampled. Figure 1a and d shows, respectively, the aortic and pulmonary valve immediately after being thawed. The valves were opened along the axis as shown in Figure 1b and e. In these two figures, the leaflets are attached to the sinuses; however, they were removed from the valve before leaflet samples were cored out. Each circular hole, shown in Figure 1c and f, was made when a sample was cored out.

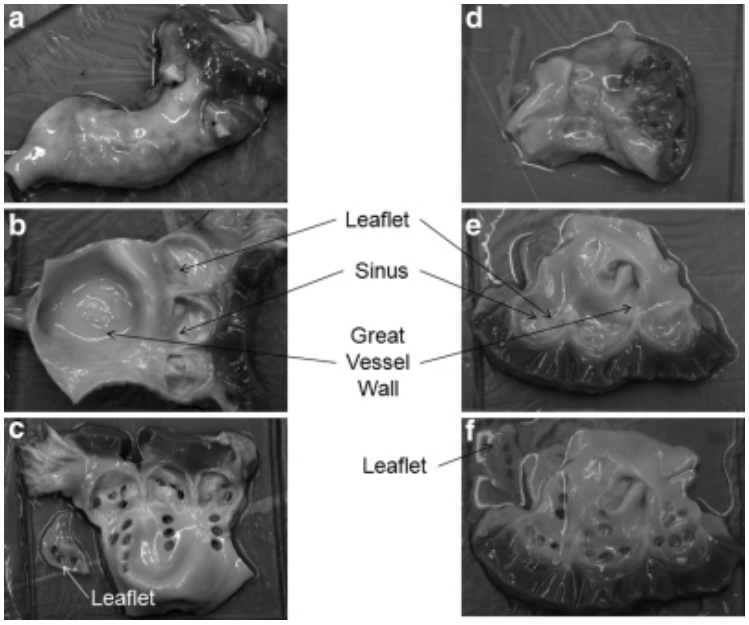

FIG. 1.

Cryopreserved aortic valve (04-2155) and pulmonary valve (06-4709). **(a)** The aortic valve immediately after being thawed. **(b)** The aortic valve cut to open along the axis. The leaflets attached to the sinuses. They were cut from the valve before samples are cored out. **(c)** Thin cylindrical samples were cored from the leaflet, sinus, and great vessel wall of this aortic valve, as shown by the circular holes. **(d)** The pulmonary valve immediately after being thawed. **(e)** The valve cut to open along the axis. The leaflets are attached to the sinuses. They were cut from the valve before samples are cored out. **(f)** Thin cylindrical samples were cored from the leaflet, sinus, and great vessel wall of this pulmonary valve, as shown by the circular holes.

Diameters of the thin cylindrical samples were in the range 3–5 mm. Thicknesses of the samples were quite different, depending on the species, the subject, and which region the samples were taken from. For the same species, samples from aortic valves are thicker than those from pulmonary valves. In general, the leaflet samples were ~0.2–0.4 mm thick and samples from the sinus and great vessel wall

were ~1–2 mm thick. Samples from the great vessel wall were slightly thicker than those from the sinus. During testing, the temperature of the environmental chamber is maintained at 34°C–37°C, with relative humidity above 90%.

Experimental method

For torsional wave experiments,[20,21] a thin, cylindrical sample of soft material is placed between two hexagonal plates: the "top plate" and "bottom plate" shown in the inset of Figure 2. These two plates are aligned vertically, sharing a common axis. The bottom plate is mounted on the drive shaft of a galvanometer that can oscillate about its axis at angles up to±6° and frequencies up to 2500 Hz. To ensure that the shear strains in the sample are sufficiently small for linear viscoelasticity to be a satisfactory approximation, the imposed rotations are maintained to be less than±0.2°. This assembly is enclosed in an environmental chamber in order to provide *in vivo* conditions. Compared with the soft viscoelastic sample, the acrylic bottom and top plates can be considered to be rigid. Therefore, when the bottom plate is oscillated, a torsional wave propagates up and down through the thickness of the sample. Based on the wave analysis described previously,[20,21] the rotation of the top plate $\theta(h, t)$ can be expressed as

$$\theta(h,t) = M(\omega_0, h)\theta_0 \cos(\omega_0 t - \phi(\omega_0, h)) \quad (1)$$

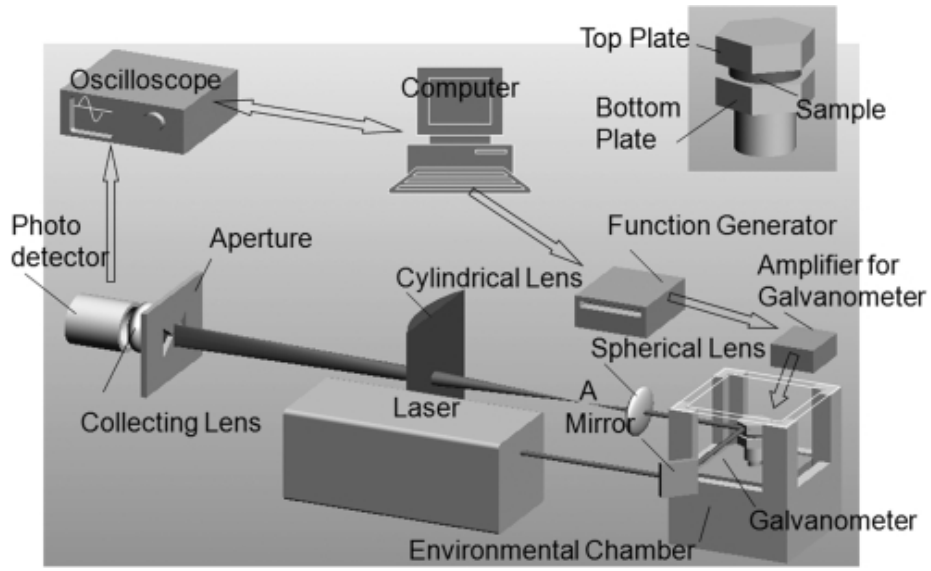

FIG. 2.

Torsional wave experimental setup.

in which h is the thickness of the sample; ω_0 and θ_0 are the frequency and amplitude of the rotation of the bottom plate, respectively; and $M(\omega_0, h)$ and $\phi(\omega_0, h)$ are, respectively, the amplification factor and the phase shift that relate the amplitude and phase of the motion of the top plate to that of the bottom plate. The amplification factor and phase shift are given by

(2)

$$M = \frac{c}{\sqrt{c^2[\cos^2(\xi\alpha) + \sinh^2(\xi\beta)] + d^2[\cosh^2(\xi\beta) - \cos^2(\xi\alpha)] + cd(\beta\sinh(2\xi\beta) - \alpha\sin(2\xi\alpha))}}$$

and

$$\tan(\phi(\omega_0)) = \frac{(c\sin(\xi\alpha) + d\alpha\cos(\xi\alpha))\sinh(\xi\beta) + d\beta\sin(\xi\alpha)\cosh(\xi\beta)}{(c\cos(\xi\alpha) - d\alpha\sin(\xi\alpha))\cosh(\xi\beta) + d\beta\cos(\xi\alpha)\sinh(\xi\beta)} \quad (3)$$

where

$$c = c(\omega_0) \equiv J\sqrt{|G^*(\omega_0)|\rho} \quad (4a)$$

$$d = d(\omega_0) \equiv \rho_0 I_0 \omega_0 \quad (4b)$$

$$\xi = \omega_0 h\sqrt{\frac{\rho}{|G^*(\omega_0)|}} \quad (4c)$$

$$\alpha = \cos\left(\frac{\delta(\omega_0)}{2}\right) \text{ and } \beta = \sin\left(\frac{\delta(\omega_0)}{2}\right) \quad (4d)$$

in which the complex shear modulus $G^*(\omega_0)$ of the sample is expressed in terms of its magnitude $|G^*(\omega_0)|$ and its loss angle $\delta(\omega_0)$.

If the responses $M(\omega_0, h)$ and $\phi(\omega_0, h)$ are measured over a range of frequencies, then the moduli $|G^*(\omega_0)|$ and $\delta(\omega_0)$ can be estimated by means of regression analysis. Values for these two parameters are readily obtained using an Excel spreadsheet and minimizing the differences between calculated and measured values of the amplification factor. Once $|G^*|$ and δ are determined, the storage modulus G' and the loss modulus G'' can be calculated from $G'=|G^*|\cos(\delta)$ and $G''=|G^*|\sin(\delta)$.

The oscillation of the galvanometer is driven by a frequency generator that steps through a sequence of frequencies from a minimum frequency, f_{min}, to a maximum frequency, f_{max}, with steps of Δf. At each frequency, the amplitudes of the rotation of the top and bottom plates are measured by an optical lever technique as shown in Figures 2 and 3.[20,21] To measure the sample geometry, a picture of the sample with both top and bottom plates was taken before and after each test. Using Adobe Photoshop, the ratios of the thickness and the width of a facet of the top plate to the thickness and diameter of a sample can be measured, respectively. With the measurement of the thickness and width of the facet of the top plate, the thickness and diameter of the sample can be calculated.

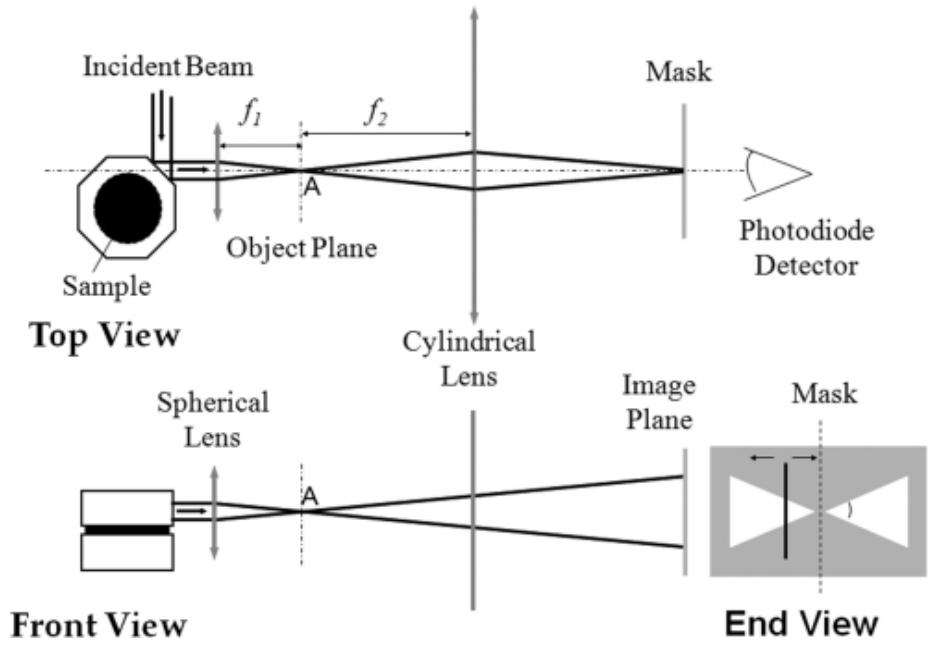

FIG. 3.

Optical layout of torsional wave experiments.

The measured amplification factors are determined at several frequencies. In Figure 4, the top trace is the measured rotation of the top plate and the bottom trace is the measured rotation of the bottom plate. Every two periods of the sinusoidal wave form corresponds to one period of the oscillation of the corresponding plate. As the frequency is stepped up, the angle of rotation of the top plate increases and that of the bottom plate stays almost the same or even decreases a little. Eventually, the amplification factor reaches a peak value at the resonance frequency, f_{peak}, and then decreases.

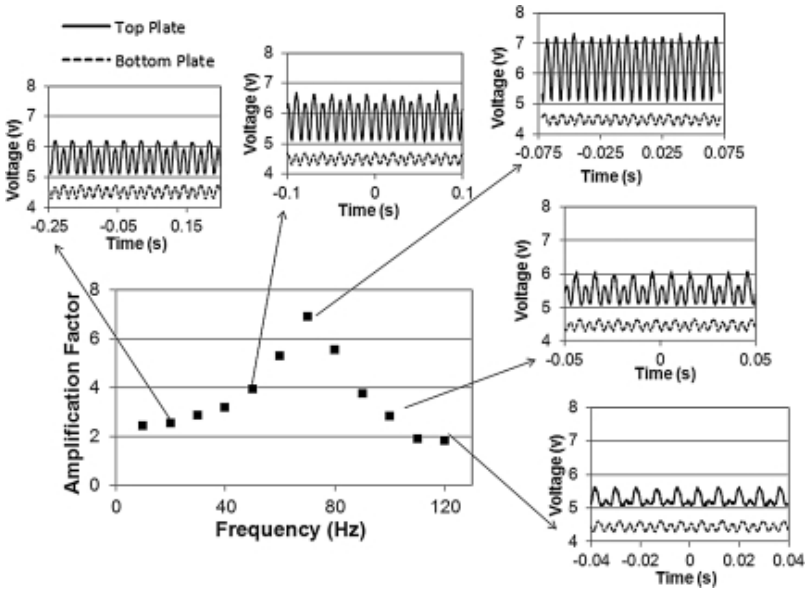

FIG. 4.

Typical output of the amplification factors at successive frequencies, with records of the wave traces at several frequencies.

Statistical analysis method

As shown in the next part, the test results indicate little frequency dependence of the viscoelastic properties over the tested frequency ranges. For each species, the characteristic viscoelastic moduli for each type of tissue (leaflet, sinus, and great vessel wall) are obtained by averaging results of tests on all tissues of the same type, from all the valves. For example, four cryopreserved human aortic valves were tested. For each aortic valve, there are three leaflets. From each leaflet, two to three samples are tested. Therefore, the viscoelastic moduli of the leaflets for cryopreserved human aortic valves are values averaged over all 35 samples. The error bar represents the confident interval at 95% confidence level. To compare the stiffnesses of tissues of different types, nonparametric methods, including Kruskal–Wallis and Mann–Whitney *U* tests, were used to analyze the data. Stiffnesses of the two types of tissues being compared are said to be statistically different for $p<0.01$; otherwise, their stiffnesses are interpreted as being statistically the same.

Results

Figure 5 shows representative curves of frequency dependence of amplification factors for samples from a human cryopreserved aortic valve. From these plots, it is evident that the linear viscoelastic wave analysis provides a remarkably good fit to the observed frequency dependence of the amplification factor over a range of frequencies spanning the peak. The inserts in Figure 5 show the samples sandwiched between the top and bottom plates.

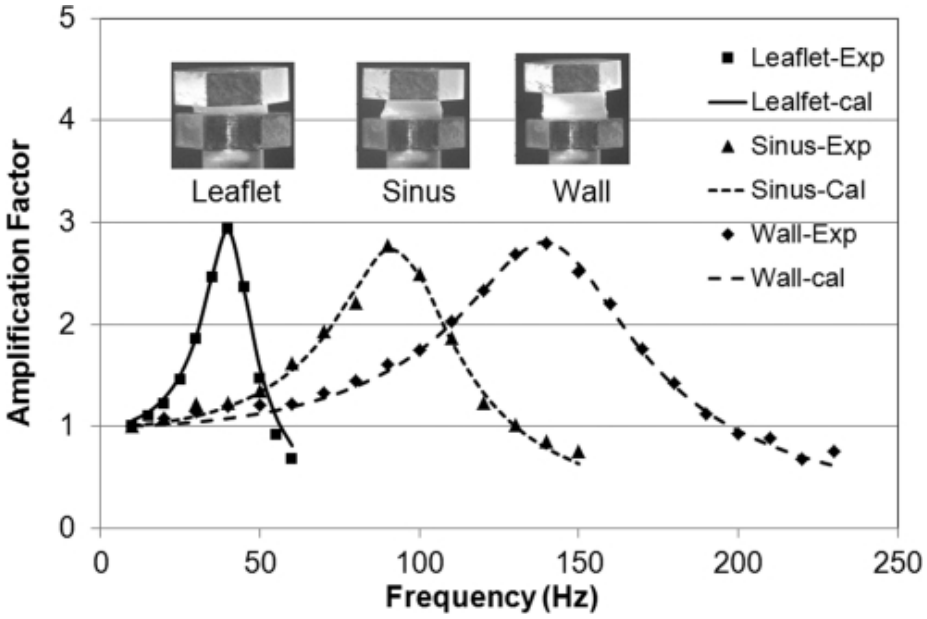

FIG. 5.

Typical fit of the experimental results with torsional wave theory for leaflet, sinus, and great vessel wall of a cryopreserved aortic valve from a human. The symbols show the experimental results and the curves show the fitted results from the wave analysis.

For the same top and bottom plates, the resonant frequency depends on the sample size (thickness and diameter) and the properties of the sample. The frequency range is usually from 50 to 100 Hz for leaflets and 100 to 150 Hz for samples from the sinus and great vessel wall. Test results indicate little frequency dependence of the viscoelastic properties over these frequency ranges. Moreover, as indicated earlier, age and gender of the samples are not main factors investigated in this pilot report. To compare the mechanical response of the tissues before and after decellularization for different species, we averaged the test results of each type tissue from the samples at three positions of each valve and for all tested fresh or decellularized valves to obtain characteristic results for the various species. Therefore, the experimental results of human samples presented here represent only average behavior. They are not representative of specific cohorts of patients in specific age ranges. Storage moduli determined for all tissues tested are tabulated in Table 3. The *p*-values from the statistical analysis of whether moduli for natural tissues and decellularized tissues are statistically comparable are also shown (Table 3).

Table 3.

Storage Modulus of All Types of Tissues

			Storage modulus (kPa)		
Sample			***Fresh***	***Decellularized***	**p-*Value***
Ovine	AV	Leaflet	0.350±0.045	0.296±0.0278	0.052
		Sinus	4.48±0.72	5.93±0.88	0.075
		Wall	5.03±0.97	5.37±0.86	0.596
	PV	Leaflet	0.337±0.095	0.373±0.110	0.775
		Sinus	2.851±0.600	1.057±0.172	0.001
		Wall	3.003±0.474	1.267±0.208	0.001
Baboon	AV	Leaflet	1.297±0.495	1.54±0.404	0.437
		Sinus	9.01±1.457	12.94±0.3045	0.034
		Wall	12.2±3.693	10.37±2.095	0.401
	PV	Leaflet	0.822±0.216	2.348±0.462	0.001
		Sinus	2.85±0.829	4.80±1.17	0.037
		Wall	5.29±1.83	4.70±1.14	0.566
Human	AV	Leaflet	0.545±0.079	0.48±0.087	0.368
		Sinus	9.27±1.214	7.32±0.71	0.007
		Wall	10.52±1.07	8.59±0.80	0.011
	PV	Leaflet	0.228±0.022	0.351±0.046	0.001
		Sinus	2.85±0.40	2.52±0.29	0.316
		Wall	3.47±0.40	2.88±0.29	0.119

Figure 6 shows the experimental results for the three types of tissues for valves from sheep. Leaflet tissues are shown to be very pliable for both aortic and pulmonary valves. Stiffnesses of sinus and great vessel wall tissues are comparable ($p>0.122$); however, the stiffness of pulmonary valve tissues tends to be lower than that of aortic valve tissues ($p<0.009$). As shown in Table 3, the principal effect of decellularization is that the stiffnesses of sinus and great vessel wall tissues of pulmonary valves are significantly reduced ($p<0.01$). Leaflet stiffness is essentially the same for both aortic and pulmonary valves, either fresh or decellularized. Similarly, tan(δ) values are essentially the same for all tissues, either fresh or decellularized.

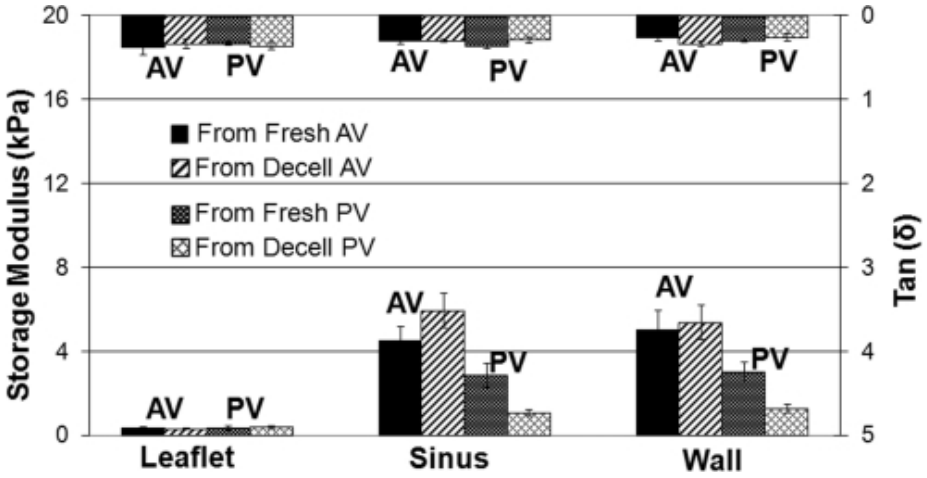

FIG. 6.

Experimental results of the viscoelastic properties of the tissues of aortic and pulmonary valves from sheep. The bars at the bottom and the top of the plot represent, respectively, the averaged storage modulus and Tan(δ), where δ is the loss angle. The error bar shows the range of the distribution of the results that fall within confident interval at 95% confidence level. AV, aortic value; PV, pulmonary valve.

Experimental results for baboon tissues are shown in Figure 7. In the baboon, both aortic and pulmonary valve leaflet tissues exhibit much lower stiffness than tissue from the sinuses and great vessel walls (p<0.002). Additionally, the pulmonary valve sinus and great vessel wall tissues exhibit lower stiffness than for the correspondent aortic valve tissues (p<0.007). Figure 7 and Table 3 show that except for leaflets of pulmonary valves, which tend to be stiffer after being decellularized (p<0.001), decellularization does not appear to have a significant effect on the stiffness of any of the baboon tissues (p>0.034). Tan(δ) values are essentially the same for all tissues and comparable to those for sheep.

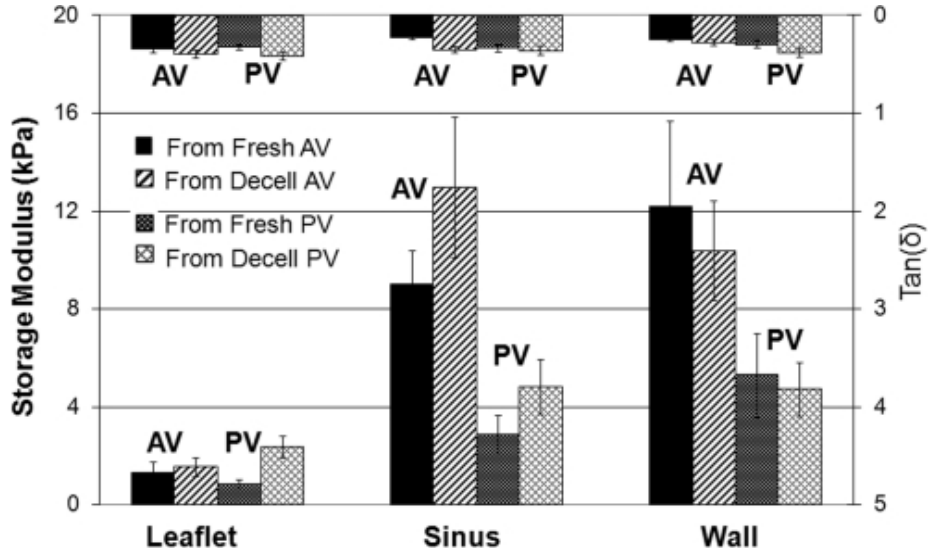

FIG. 7.

Experimental results of the viscoelastic properties of the tissues of aortic and pulmonary valves from baboon (labels are the same as in Fig. 6).

Storage modulus and loss tangent values for human heart valve tissues are shown in Figure 8. For human valves, the “fresh” tissues were cryopreserved as described earlier. Similar to the baboon, human leaflet tissue from both aortic and pulmonary valves exhibit much lower stiffness than tissues from the sinus and great vessel wall ($p<0.001$). Also, sinus and great vessel wall tissues from aortic valves are stiffer than those from pulmonary valves ($p<0.001$). As shown in Figure 8 and Table 3, after being decellularized, the stiffness of pulmonary valve leaflets increased ($p<0.001$), whereas the stiffness of decellularized sinus of aortic valve decreased ($p<0.007$). For the other tissues from human heart valves, decellularization does not appear to have a significant effect on their stiffnesses ($p>0.01$). Tan(δ) values do not vary significantly over the three types of tissues and appear to be comparable to those for sheep and baboon.

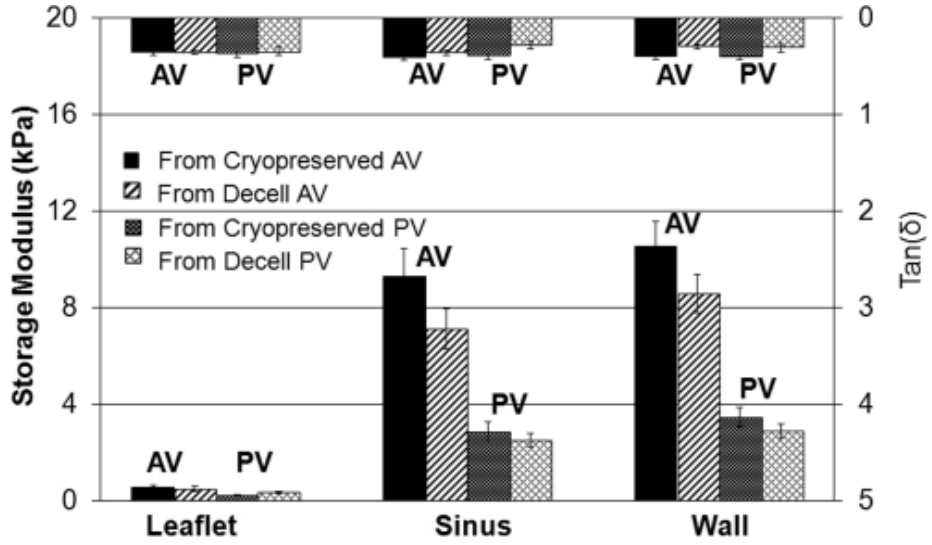

FIG. 8.

Experimental results of the viscoelastic properties of the tissues of aortic and pulmonary valves from human (labels are the same as in Fig. 7).

For comparisons between different species, the measured viscoelastic properties for fresh/cryopreserved sheep, baboon, and human aortic and pulmonary valve tissues are shown in Figure 9a and b, respectively. Figure 9a clearly shows that the viscoelastic properties of the tissues from human aortic valves are closest to those of baboon. Stiffnesses for aortic valve tissues from sheep are significantly lower than those of the other two species ($p<0.001$), except the leaflet, which is comparable to that from human ($p>0.019$), but softer than that from baboon ($p<0.001$). No significant differences were observed in the viscoelastic properties of pulmonary valve tissues between these three species, except that the storage modulus of the leaflet and great vessel wall are slightly higher in the baboon than in the other two species.

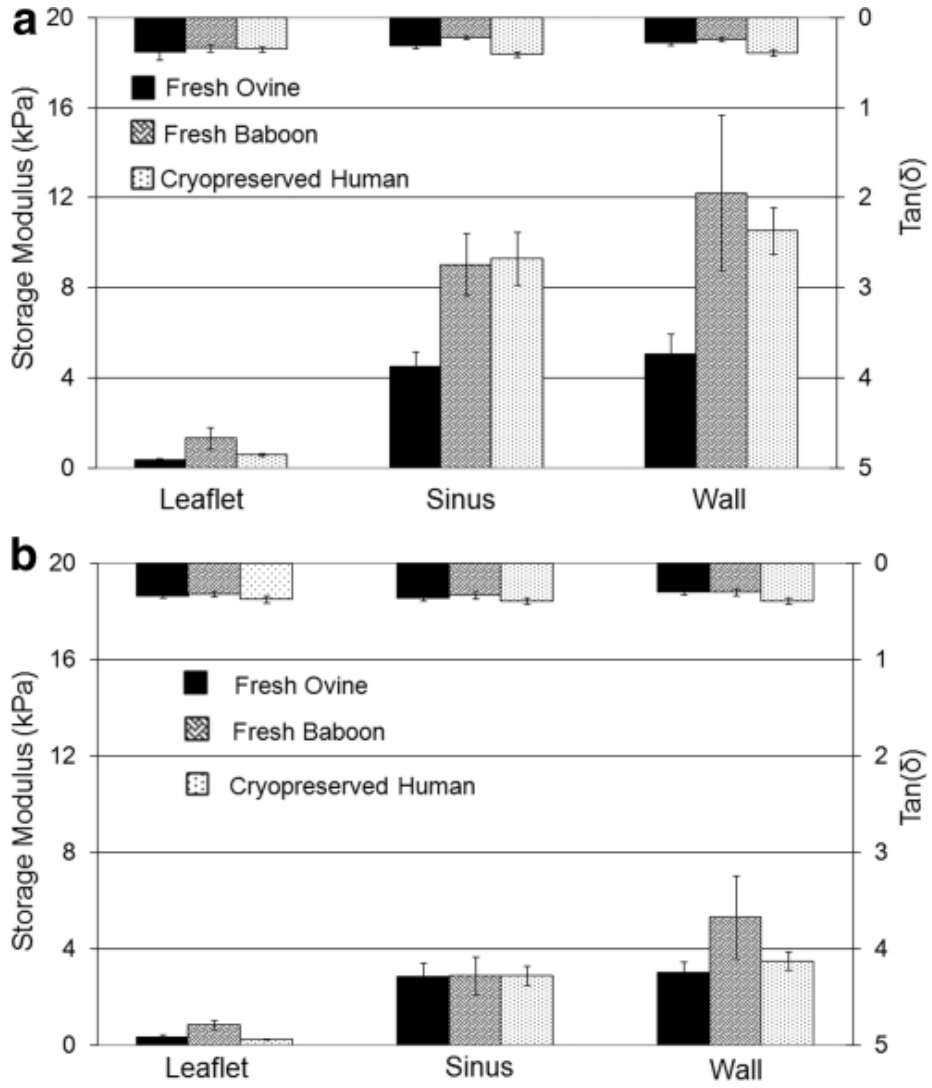

FIG. 9.

(a) Comparison of viscoelastic properties of fresh aortic valves from sheep and baboon and from cryopreserved human samples. **(b)** Comparison of viscoelastic properties of fresh pulmonary valves from sheep and baboon and from cryopreserved human samples.

Discussion

The first human clinical surgical use of fresh aortic valve homografts transplanted into the descending thoracic aorta for clinical amelioration of the consequences of native aortic valve insufficiency was reported by Gordon Murray in 1956.[22] As manufactured prosthetic valves gradually evolved in design and range of choices, the use of homograft valves began to decline, not due to performance, but rather as a consequence of logistics, banking, and tissue transport issues.[23] In the 1980s and 1990s, cardiovascular allograft tissues became increasingly available, primarily as cryopreserved valves with variably retained native cell viability. Especially for pediatric use, the surgical and specific hemodynamic advantages of homograft semilunar cardiac valves have been recognized.

Although these transplanted valves performed well in the short to mid term, they have been associated with ultimate fibrosis, calcification, and failure in a significant proportion of cases, especially for infants and young children, for whom retained growth and repair functions would be ideal.[23] Ganguly *et al.* have evaluated the pattern of homograft failure and the quality of life in patients after homograft implantation.[24] They found the performance status of 60% of respondents to be good, 20% to be moderate, and 20% to be poor. Eleven patients (18.9%) required subsequent redo valve replacement after initial homograft insertion (pulmonary=6, aortic=5). Therefore, there are continuing efforts to develop "tissue-engineered" heart valves to achieve viability combined with relative or actual immune tolerance with the thought that this would retain the outstanding engineering design of the native semilunar valve while avoiding the inevitable destructive foreign body reaction to transplanted proinflammatory materials. Simon *et al.* have reported early failure of the tissue-engineered porcine heart valve in pediatric patients.[25] In fact, this case and some other experiments demonstrate that the lowest level of stimulation was with thoroughly "decellularized" human tissues.[26] Therefore, one conceptual path to an autologous recellularized tissue-engineered valve is to start with an acellular allogeneic ECM scaffold of proven design derived from decellularized human allograft. Subsequent *ex vivo* or *in vivo* recellularization could establish a native multicellular host population that organizes as a living, functioning heart valve tissue that can grow and remodel, potentially leading to improved wear properties.

However, appealing theoretically, there is risk that any decellularization process may result in hazardous alterations of physical properties of the valve itself. Such material and performance degradations need to be carefully defined, measured, and related to appropriate standards derived from similar measurements of functioning human valves. Critical material properties of semilunar heart valves involve the inherent viscoelasticity, evidenced by the known frequency dependence of the functional components of the valves (leaflets, sinus walls, and great vessel wall above the valve).[27]

There are few investigations focused on the shear properties of heart valve tissues; even fewer reports are on the viscoelastic shear properties of cardiovascular materials. Most available reports on the biomechanical properties of aortic/pulmonary heart valve tissue address their tensile and flexure behavior. Thubrikar *et al.*[2] have investigated the mechanical properties of aortic valve leaflets from dogs. They measured the tensile stress–strain curve both *in vivo* and *in vitro.* Vesely and Boughner[3] have measured the bending stiffness of porcine xenograft leaflets. Sacks and his colleagues have investigated the biaxial and the flexural properties of leaflets from fresh porcine heart valves.[4–9] With data from all of these experiments, Sacks[10] constructed a structural constitutive model to describe the behavior of leaflets. As the biomechanical properties of the heart valve leaflet have been well characterized using conventional techniques, less mechanical test data are available for tissues from different parts of the heart valve. Most available data on the sinus and great vessel wall of both aortic valves and pulmonary valves are inferred from measurements of tissues from arterial walls. Hayashi *et al.*[11] have used uniaxial and biaxial tension to get the basic mechanical properties of calf arterial walls. Silver *et al.*[12–15] have obtained the "pressure–strain" elastic modulus and circumferential elastic modulus of arterial walls by noninvasively measuring the blood pressure vs. the diameter change of human aorta. Silver *et al.* also measured the uniaxial tension stress–strain curve and uniaxial tension incremental stress–strain curve of human aortic walls.

Storage moduli reported herein for sinus and great vessel walls under shear are approximately an order of magnitude smaller than those obtained for arterial walls by pressure–diameter measurement and uniaxial tension.[13] Differences are likely due to the strains at which the moduli are measured. The stress–strain curve of a natural tissue subjected to simple tension is nonlinear, having a very low elastic modulus in the low strain regime, increasing with progressively higher strains to a much larger value at larger strains. For arteries, the walls are in tension initially. The starting strain of the pressure–diameter

measurement corresponds to a strain of ~30%.[13] Because the tissues are very soft, elastic moduli in the low strain regime are difficult to measure accurately by uniaxial tension. Consequently, the measurements below strains of 30% are neglected. In torsional wave experiments, the maximum strain applied is ~5%, which is much smaller than for the other methods. Therefore, the storage moduli obtained by torsional wave experiments can be expected to be significantly smaller than the values obtained in other investigations.

When blood flow passes the valves, the valve tissues are working in the regime of low stresses and strains. Experiments[28–31] have shown that wall shear stress above 400 dynes/cm^2 (40 Pa) can damage the endothelial lining of the aorta, and shear stresses above 950 dynes/cm^2 can erode the endothelium from the vessel wall. Aortic wall shear stresses of ~29 dynes/cm^2 have been measured downstream of xenograft aortic valves *in vitro*.[30,31] Aortic valve leaflets are also covered with an endothelial lining. Weston *et al.*[32] have found that the maximum shear stress on the leaflets is about 79 dynes/cm^2. The shear moduli of the heart valve tissues reported herein are measured under conditions similar to those at which they function. For leaflets of heart valves in systole phase, they are stretched up to 30% deformation. Under this condition, their viscoelastic shear responses can be expected to be different from those reported here, which are measured without prestretching. However, the reported measurements provide simple and systematic comparisons to elucidate the change of mechanical properties before and after decellularization. They also provide direct comparison of differences in the mechanical properties of tissues from different species.

The procedure of cryopreservation may have some impact on the ECM structure.[33,34] However, as the fresh human heart valves are difficult to obtain and cryopreserved heart valves are still the widely used homografts for implantation, we compared the viscoelastic properties of cryopreserved human heart valve tissues before and after decellularization. Several reports of the effects of decellularization on the quasistatic mechanical properties of heart valve tissues are available in the literature.[35–41] Seebacher *et al.* reported no change in the strength of porcine pulmonary valve conduits in uniaxial tension following decellularization, though stiffness values were not reported.[35] Korossis *et al.* found no difference in the tensile strength of porcine aortic valve leaflets but did report a significant decrease in stiffness within the elastin-dominated region of the stress–strain curve.[36] Liao *et al.* investigated the effects of multiple decellularization protocols on the biomechanics of porcine aortic valve leaflets under flexural and planar biaxial loading conditions. The authors reported decreased flexural stiffness regardless of the decellularization protocol used but also reported increases in areal strain and tangent modulus under biaxial loading conditions. The relative magnitude of these changes varied with decellularization protocol.[37] Hydrodynamic performance of heart valves treated by different decellularization protocols has also been investigated. Dohmen *et al.* have made *in vitro* measurements of the hydrodynamics of decellularized pulmonary porcine valves and compared with glutaraldehyde and polyurethane heart valves.[38] They found that decellularized pulmonary porcine valves showed the same excellent performance as polyurethane valve prosthesis. Recently, Bottio *et al.* have investigated the hydrodynamic behavior of intact porcine aortic roots, both before and after decellulariztion.[39] They have used four decellularization protocols, TRI-COL, TRI-DOC, sodium dodecyl sulfate (SDS) 0.03%, and SDS 0.1%. They found that, except for SDS 0.03%, the other three protocols modified the systolic and diastolic functions of intact porcine aortic root.

In this report, because the fresh tissues and the decellularized tissues are not from the same valve, comparisons between fresh and decellularized tissues are not direct. However, the comparison between the results averaged over three or four fresh/cryopreserved and decellularized valves appears to provide a statistically significant indication of the effect of decellularization. Statistical analysis (see Table 3) shows that for most (i.e., 13 of 18) statistical comparisons of our experimental results on fresh/cryopreserved and decellularized samples, the decellularization used in this series of experiments

did not cause significant changes in stiffness. The exceptions are ovine—sinus and great vessel wall of pulmonary valves; baboon—leaflet of pulmonary valves; and human—sinus of aortic valves and leaflet of pulmonary valves. Even for those tissues whose stiffnesses have statistically changed, the magnitude of these changes may not be large enough to cause any functional consequences. Quinn *et al.*[19] reported comparable hemodynamic performance between cryopreserved and decellularized pulmonary valves in a 20-week ovine surgical model. These results suggest that ECM structural proteins, not cells, are the dominant contributors to the passive viscoelastic properties of semilunar valves and those ECM properties are typically not altered by decellularization. By experimental design, this method cannot test for active cellular contractility but may assess the passive contribution of cell-based proteins in the "native cryopreserved" valves.[42] Clearly, it is important to consider the effects of a specific decellularization protocol on the mechanical behavior of heart valves intended for use as tissue-engineering constructs. However, because of differences in decellularization protocols and biomechanical properties measured, direct comparison with previous reports cannot be made.

Conclusions

1. For sheep, baboon, and human—and for both aortic and pulmonary valves—the leaflet is softer than the sinus and the great vessel wall. The latter two tissues have similar stiffness.
2. For the same species, tissues from aortic valves are stiffer than the corresponding tissues from pulmonary valves.
3. Loss angles are similar for all tissue samples.
4. Regardless of species, the decellularization process used here causes only modest changes in viscoelastic properties.

Acknowledgments

This research was supported by Brown University and by Children's Mercy Hospital and NIH–SNPRC Base Grant No. P51RR013986-11, Southwest National Primate Research Center (SNPRC) Grants-in-Aid "Bioengineered Heart Valves: Baboon Implant Feasibility Study."

Disclosure Statement

No competing financial interests exist.

References

1. Sacks M.S. Merryman W.D. Schmidt D.E. On the biomechanics of heart valve function. J Biomech. 2009;42:1804. [PMC free article] [PubMed] [Google Scholar]

2. Thubrikar M.J. Aouad J. Nolan S.P. Comparison of the in vivo and in vitro mechanical properties of aortic valve leaflets. J Thorac Cardiovasc Surg. 1986;92:29. [PubMed] [Google Scholar]

3. Vesely I. Boughner D. Analysis of the bending behavior of porcine xenograft leaflet and of natural aortic valve material: bending stiffness, neutral axis and shear measurements. J Biomech. 1989;22:655. [PubMed] [Google Scholar]

4. Grashow J.S. Yoganathan A.P. Sacks M.S. Biaxial stress-stretch behavior of the mitral valve anterior leaflet at physiologic strain rates. Ann Biomed Eng. 2006;34:315. [PubMed] [Google Scholar]

5. Grashow J.S. Sacks M.S. Liao J. Yoganathan A.P. Planar biaxial creep and stress relaxation of the mitral valve anterior leaflet. Ann Biomed Eng. 2006;34:1509. [PubMed] [Google Scholar]

6. Stella J.A. Liao J. Sacks M.S. Time-dependent biaxial mechanical behavior of the aortic heart valve leaflet. J Biomech. 2007;40:3169. [PMC free article] [PubMed] [Google Scholar]

7. Stella J.A. Sacks M.S. On the biaxial mechanical properties of the layers of the aortic valve leaflet. J Biomech Eng. 2007;129:757. [PubMed] [Google Scholar]

8. Merryman W.D. Huang H.S. Schoen F.J. Sacks M.S. The effects of cellular concentration on aortic valve leaflet flexural stiffness. J Biomech. 2006;39:88. [PubMed] [Google Scholar]

9. Mirnajafi A. Raymer J.M. McClure L.R. Sacks M.S. The flexural rigidity of the aortic valve leaflet in the commissural region. J Biomech. 2006;39:2966. [PubMed] [Google Scholar]

10. Sacks M.S. Incorporation of experimentally-derived fiber orientation into a structural constitutive model for planar collagenous tissues. J Biomech Eng. 2003;125:280. [PubMed] [Google Scholar]

11. Hayashi K. Experimental approaches on measuring the mechanical properties and constitutive laws of arterial walls. J Biomech Eng. 1993;115:481. [PubMed] [Google Scholar]

12. Cilver F.H. Horvath I. Foran D.J. Viscoelasticity of the vessel wall: the role of collagen and elastic fibers. Crit Rev Biomed Eng. 2001;29:279. [PubMed] [Google Scholar]

13. Silver F.H. Snowhill P.B. Foran D.J. Mechanical behavior of vessel wall: a comparative study of aorta, vena cava, and carotid artery. Ann Biomed Eng. 2003;31:793. [PubMed] [Google Scholar]

14. Kalath S. Tsipouras P. Silver F.H. Non-invasive assessment of aortic mechanical properties. Ann Biomed Eng. 1986;14:513. [PubMed] [Google Scholar]

15. Dunn M.G. Silver F.H. Viscoelastic behavior of human connective tissues: relative contribution of viscous and elastic components. Connect Tissue Res. 1983;12:59. [PubMed] [Google Scholar]

16. Hopkins R.A. Hammon J.W., Jr. McHale P.A. Smith P.K. Anderson R.W. Pulmonary vascular impedance analysis of adaptation to chronically elevated blood flow in the awake dog. Circ Res. 1979;45:267. [PubMed] [Google Scholar]

17. Hopkins R.A. Hammon J.W., Jr. McHale P.A. Smith P.K. Anderson R.W. An analysis of the pulsatile hemodynamic responses of the pulmonary circulation to acute and chronic pulmonary venous hypertension in the awake dog. Circ Res. 1980;47:902. [PubMed] [Google Scholar]

18. Hopkins R.A. Cardiac Reconstructions with Allograft Tissues. New York: Springer-Verlag; 2005. [Google Scholar]

19. Quinn R.W. Hilbert S.L. Bert A.A. Drake B.W. Bustamante J.A. Fenton J.E. Moriarty S.J. Neighbors S.L. Lofland G.K. Hopkins R.A. Performance and morphology of decellularized pulmonary valves implanted in juvenile sheep. Ann Thorac Surg. 2011;92:131. [PubMed] [Google Scholar]

20. Clifton R.J. Jiao T. Bull C. Methods and apparatus for measuring the viscoelastic response of vocal fold tissues and scaffolds across a frequency range. United States Patent. 2004. p. 7387032.

21. Jiao T. Farran A. Jia X. Clifton R.J. High frequency measurements of viscoelastic properties of hydrogels for vocal fold regeneration. Exp Mech. 2009;49:235. [PMC free article] [PubMed] [Google Scholar]

22. Murry G. Homologous aortic valve segment transplants a surgical treatment for aortic and mitral insufficiency. Angiology. 1956;7:466. [PubMed] [Google Scholar]

23. Hopkins R.A. Tissue engineering of heart valves: decellularized valve scaffolds. Circ Am Heart Assoc. 2005;111:2712. [PubMed] [Google Scholar]

24. Ganguly G. Akhunji Z.A. Neethling W.M. Hodge A.J. Homograft aortic valve replacement—the experience of one unit. Heart Lung Circ. 2004;13:161. [PubMed] [Google Scholar]

25. Simon P. Kasimir M.T. Seebacher G. Weigel G. Ullrich R. Salzer-Muhar U. Rieder E. Wolner E. Early failure of the tissue engineered porcine heart valve SYNERGRAFT in pediatric patients. Eur J Cardiothorac Surg. 2003;23:1002. [PubMed] [Google Scholar]

26. Hopkins R.A. From cadaver harvested homograft valves to tissue-engineered valve conduits. Prog Pediatr Cardiol. 2006;21:137. [Google Scholar]

27. Domkowski P.W. Messier R.H. Cockerham J.T. Kot P.A. Diodato L.H. Hopkins R.A. Relationship of hydraulic impedance and elasticity in the pulmonary artery of maturing newborn pigs. J Surg Res. 2001;100:116. [PubMed] [Google Scholar]

28. Fry D.L. Certain histological and chemical response of the vascular interface to acutely induced stress in the aorta of the dog. Circ Res. 1969;24:93. [PubMed] [Google Scholar]

29. Fry D.L. Acute vascular endothelial changes associated with increase blood velocity gradiens. Circ Res. 1968;22:165. [PubMed] [Google Scholar]

30. Nandy S. Tarbbell J.M. Flush mounted hot film anemometer measurements of the wall shear stress distal to a tri-leaflet valve for newtonian and non-newtonian blood analog fluids. Biorheology. 1987;24:483. [PubMed] [Google Scholar]

31. Walburn F.J. Stein P.D. Wall shear stress during pulsatile flow distal to a normal porcine aortic valve. J Mech. 1985;17:97. [PubMed] [Google Scholar]

32. Weston M.W. LaBorde D.W. Yoganathan A.P. Estimation of the shear stress on the surface of an aortic valve leaflet. Ann Biomed Eng. 1999;27:572. [PubMed] [Google Scholar]

33. Schenke-layland K. Madershahian N. Riemann I. Starcher B. Halbhuber K. Konig K. Stock U.A. Impact of cryopreservation on extracellular matrix structures of heart valve leaflet. Ann Thorac Surg. 2006;81:918. [PubMed] [Google Scholar]

34. Lisy M. Pennecke J. Brockbank K.G.M. Fritze O. Schleicher M. Schenke-layland K. Kaulitz R. Weber C.N. Braun J. Mueller K.E. Fend F. Scheunert T. Gruber A.D. Albes J.M. Huber A.J. Stock U.A. The performance of ice-free cryopreserved heart valve allografts in an orthotropic pulmonary sheep model. Biomaterials. 2010;31:5306. [PubMed] [Google Scholar]

35. Seebacher G. Grasl C. Stoiber M. Stoiber M. Rieder E. Kasimir M.-T. Dunkler D. Simon P. Weigel G. Schima H. Biomechanical properties of decellularized porcine pulmonary valve conduits. Artif Organs. 2008;32:28. [PubMed] [Google Scholar]

36. Korossis S.A. Booth C. Wilcox H.E. Watterson K.G. Kearney J.N. Fisher J. Ingham E. Tissue engineering of cardiac valve prostheses II: biomechanical characterization of decellularized porcine aortic heart valves. J Heart Valve Dis. 2002;11:463. [PubMed] [Google Scholar]

37. Liao J. Joyce E.M. Sacks M.S. Effects of decellularization on the mechanical and structural properties of the porcine aortic valve leaflet. Biomaterials. 2008;29:1065. [PMC free article] [PubMed] [Google Scholar]

38. Dohmen P.M. Scheckel M. Stein-konertz M. Erdbruegger W. Affeld K. Konertz W. In vitro hydrodynamics of a decellularized pulmonary porcine valve, compared with a glutaraldehyde and polyurethane heart valve. Int J Artif Organs. 2002;25:1089. [PubMed] [Google Scholar]

39. Bottio T. Tarzia V. Lin C.D. Buratto E. Rizzoli G. Spina M. Gandaglia A. Naso F. Gerosa G. The changing hydrodynamic performance of the decellularized intact porcine aortic root: Considerations on in-vitro testing. J Heart Valve Dis. 2010;19:485. [PubMed] [Google Scholar]

40. Elkins R.C. Dawson P.E. Goldstein S. Walsh S.P. Black K.S. Decellularized human valve allografts. Ann Thorac Surg. 2001;71:S428. [PubMed] [Google Scholar]

41. Zhou J. Fritze O. Schleicher M. Wendel H. Schenke-Layland K. Harasztosi C. Hu S. Tock U.A. Impact of heart valve decellularization on 3-D ultratructure, immunogenicity and thrombogenicity. Biomaterials. 2010;31:2549. [PubMed] [Google Scholar]

42. Merryman W.D. Youn I. Lukoff H.D. Krueger P.M. Guilak F. Hopkins R.A. Sacks M.S. Correlation between heart valve interstitial cell stiffness and transvalvular pressure: implications for collagen biosynthesis. Am J Physiol Heart Circ Physiol. 2006;290:H224. [PubMed] [Google Scholar]

Articles from Tissue Engineering. Part A are provided here courtesy of **Mary Ann Liebert, Inc.**